PFC/JA-85-32

Ripple Stabilized High β Plasma with Conducting Wall in a Simple Mirror

Xing Zhong Li*; Jay Kesner; Linda LoDestro**

September 1985

Plasma Fusion Center
Massachusetts Institute of Technology
Cambridge, Massachusetts 02139 USA

*Permanent Address: Modern Physics Institute, Department of Physics
Tsinghua University, Beijing, China.

**Lawrence Livermore National Laboratory, Livermore, CA 94550.

Submitted for publication in: Nuclear Fusion.

Ripple Stabilized High β Plasma with Conducting Wall in a Simple Mirror

Xing Zhong Li*, Jay Kesner, Linda LoDestro**

Abstract

A simple magnetic mirror may be MHD stable, provided that (1) a certain length of magnetic field has a series of ripples in it, (2) for the isotropic pressure the plasma beta value is higher than 50% and (3) the conducting wall is very close to the plasma surface. The theory and its physical picture are discussed. A Sturm-Liouville form is present with the numerical results. For the application to Tara reactor, the rippled magnetic field may be generated by ferromagnetic rings. The implication for a blanket design is discussed.

*Permanent Address: Modern Physics Institute, Department of Physics
Tsinghua University, Beijing, China.

**Lawrence Livermore National Laboratory, Livermore, CA 94550.

1. Introduction

Recent work by Berk et.al.[1] on the possibility of the use of wall stabilization mechanisms of m = 1 curvature driven mode has stimulated a series of efforts[2] - [6] that apply this idea in a tandem mirror reactor. It has been found that the conducting wall suppresses the displacement of plasma in the unfavorable curvature region[4]. This is the essence of the wall stabilization. The line-bending effect or the response of the conducting wall in the favorable curvature region[5] is not as important in this case. In order to obtain this suppression effect for an isotropic plasma, the plasma beta (the ratio of the plasma pressure to the magnetic pressure) must be greater than 50%, and this critical beta value is a function of the mirror ratio. The higher the mirror ratio, the higher is the critical beta value. If there are some ripples in a simple mirror, then a certain plasma beta value may be high enough for the stabilization of the ripple region, but not high enough for the mirror ratio of the simple mirror. This leads to a competition between the stabilizing effect of ripple field and the unstable effect of the simple mirror. Four parameters are important to determine the result of this competition: the mirror ratio of the simple mirror, the amplitude of the ripple field, the number of the ripples, and the ratio of the ripple length to the total length of the mirror. In Section 2 we will discuss the physical picture. In Section 3, we discuss the scaling of the ripple amplitude and the number of the

ripples. In Section 4, a Sturm-Liouville form is given for the numerical calculation. In Section 5, the reactor implications are discussed.

§2. Critical β for Wall Stabilization

It has been shown that the image current inside the conducting wall can interact with the diamagnetic current inside the plasma surface to stabilize the plasma (to MHD instability). This picture is simple and intuitive, but it is less obvious whether there is a lower limit[4] [6] [7] of beta value in order to have this stabilization and why only the conducting wall in the unfavorable curvature region is essential for the stabilization[5]. Starting from Kaiser and Pearlstein's MHD equation[3], we will try to illuminate the physics for the critical beta value. The basic balloon equation in Ref. [3] is

$$\eta^2 \frac{d}{dz}\left[\Lambda \frac{d}{dz}(\eta^2\phi)\right] + \frac{d}{dz}\left[\frac{Q}{B^2}\frac{d}{dz}\phi\right] + \left(\omega^2 \frac{\rho}{B^2} - \frac{2p}{B^2}\frac{R''}{R}\right)\phi = 0 \qquad (1)$$

Here, ϕ is defined as

$$\phi = \xi(z)\sqrt{B}(z) \qquad (2)$$

$\xi(z)$ is the displacement of the plasma and B(z) is the beta corrected magnetic field. Due to the long-thin approximation and the FLR effect, $\phi(z)$ is a function of z only. Q and p are defined as

$$p = \frac{1}{2}\left(p_{||} + p_{\perp} \right) \tag{3}$$

$$Q = B_v^2 - 2p. \tag{4}$$

Here, $p_{||}$ and $p_{\perp}$ are the parallel and perpendicular pressure of the plasma, respectively; B_v is the vacuum field. η^2 is defined as

$$\eta^2 \equiv \frac{B_v}{B} \tag{5}$$

Λ represents the conducting wall effect and is defined as

$$\Lambda = \frac{r_w^2 + r_p^2}{r_w^2 - r_p^2} \tag{6}$$

Here, r_w and r_p are the radius of the conducting wall and the plasma, respectively. $\frac{R''}{R}$ is the curvature drive term, which makes plasma unstable. For an isotropic plasma we can write[4]

$$\frac{R''}{R} = \frac{1}{2\varsigma^2}\left[\left(\frac{1}{2}\tau^2 - \tau'\right) + \frac{5}{2}\sigma\tau^2\right] \tag{7}$$

The first term in the bracket is the usual vacuum curvature term

$$\frac{R''_V}{R_V} = \frac{1}{2}\left(\frac{1}{2}\tau^2 - \tau'\right) \tag{8}$$

Here

$$\tau \equiv \frac{B'_V}{B_V} \tag{9}$$

and the prime is the derivative with respect to z, the direction along the field line. ς and σ are defined as

$$\varsigma \equiv \frac{1}{\eta^2} = \sqrt{1 - \beta} \tag{10}$$

$$\sigma \equiv \frac{\beta}{1 - \beta} \tag{11}$$

Here β is the local vacuum beta

$$\beta \equiv \frac{2p}{B_V^2} \tag{12}$$

ω^2 and ρ in the equation (1) are the eigenfrequency and the mass density of the plasma. $\omega^2 > 0$ indicates stability. When the wall is very close to the plasma, $\Lambda \to \infty$; therefore, the zero order solution for ϕ is

$$\phi = \frac{1}{\eta^2} \quad ; \qquad (\text{i.e.} \, \xi = \text{constant}/RB_v) \tag{13}$$

Using the boundary condition that

$$\frac{d}{dz} \phi = 0 \quad \text{at } z = \pm L \tag{14}$$

We obtain the dispersion relation that

$$0 = \int_{-L}^{L} dz \left[\frac{1}{\eta^2} \left\{ \frac{d}{dz} \left[\frac{Q}{B^2} \frac{d}{dz} \left(\frac{1}{\eta^2} \right) \right] \right\} - \frac{2p}{B_v^2} \frac{R''}{R} + \frac{\omega^2 \rho}{B_v^2} \right]$$

or

$$0 = \int_{-L}^{L} dz \left\{ -\left[\frac{d}{dz} \left(\frac{1}{\eta^2} \right) \right]^2 - \frac{2p}{B_v^2} \frac{R''}{R} + \frac{\omega^2 \rho}{B_v^2} \right\} \tag{16}$$

Here, the isotropic pressure assumption has been used to simplify the first term. Under the long-thin approximation, using the flux conservation, we have

$$0 = \int_{-L}^{L} \frac{dz}{B} \{ - \frac{1}{R^2} [\zeta']^2 - \frac{2p}{R^2 B_v^2} \frac{R''}{R} + \frac{\omega^2 \rho}{R^2 B_v^2} \} \tag{17}$$

Since

$$(\zeta')^2 = (\zeta \sigma \tau)^2 = \frac{2p}{B_v^2} \sigma \tau^2 \tag{18}$$

we have

$$0 = \int_{-L}^{L} \frac{dz}{B} \left\{ - \left(\frac{1}{RB_v} \right)^2 2p [\sigma \tau^2] - \left(\frac{1}{RB_v} \right)^2 2p \frac{1}{2\zeta^2} [(\frac{1}{2} \tau^2 - \tau') + \frac{5}{2} \sigma \tau^2] \right.$$

$$\left. + \frac{\omega^2 \rho}{R^2 B_v^2} \right\} \tag{19}$$

In Eq. (19) the first term represents line-bending and the second term curvature. Since the ratio of the line-bending term to the curvature term is proportional to $\zeta^2 = (1 - \beta)$, it is negligible when $\beta \rightarrow 1$. Therefore, we may concentrate on the curvature drive term, which using Eq. 13 can be written as

$$Q_2 = 2p \int_{-L}^{L} \frac{dz}{B} \cdot \xi^2 \cdot \frac{R''}{R} \tag{20}$$

As is well known, in the low β case ($\beta \to 0$)

$$Q_2 = \int_{-L}^{L} \frac{dz}{(B_v R_v^2)} \frac{2p}{B_v^2} \frac{R_v''}{R_v} = \frac{1}{(B_v R_v^2)} \int_{-L}^{L} dz\, \beta \frac{R_v''}{R_v} \tag{21}$$

is always negative because of the higher β weight at the low field region. From Eqs. (20) and (7) we observe that the high β plasma brings two new features into Q_2: (1) the curvature $\frac{R''}{R}$ becomes more negative in a small midplane region due to the cusp-like effect[4]; (2) ξ^2 weighting will provide an additional suppression in the low field region when β is greater than 50%. This latter feature has been shown in Ref. [4] using the long-thin approximation. In fact, this is a general feature even if long-thin approximation is not applicable. The physical reason is that the conducting wall forces $Q_n = 0$ in the vacuum field region (Q_n is the normal component of the perturbed magnetic field), which specifies the z-dependence of the displacement $\xi(z)$.

In general,[8]

$$Q_n = (\vec{B} \cdot \nabla)\ (\vec{\xi} \cdot \vec{n}) - (\vec{\xi} \cdot \vec{n})\ \vec{n} \cdot (\vec{n} \cdot \nabla)\ \vec{B} \tag{22}$$

With, $\vec{n}$ is the unit vector in the normal direction of magnetic flux surface. $Q_n = 0$ gives

$$\frac{1}{\xi_n} \frac{\partial}{\partial l} \xi_n = \vec{n} \cdot (\vec{n} \cdot \nabla)\ \vec{b}$$

$$= (\vec{n} \cdot \nabla)\ \alpha \tag{23}$$

Here, $\frac{\partial \xi_n}{\partial l}$ is the derivative along the field line; α is the angle between field line and the z axis. Therefore,

$$\xi_o = \xi_1 \exp\left[\int_{l_1}^{l_0} dl\ (\vec{n} \cdot \nabla)\ \alpha\right] \tag{24}$$

In the Appendix A, assuming a simplified model, we show that the ratio of the displacement ξ_o at the low field region to the displacement ξ_1 at the high field region is

$$\frac{\xi_o}{\xi_1} = \left(\frac{M}{\sqrt{M_p}}\right)^{\cos^{-2}\alpha} \tag{25}$$

Here, M and M_p are the magnetic mirror ratio in the vacuum and in the plasma, respectively. In the long-thin approximation, $\alpha \to 0$, $\cos \alpha \to 1$.

$$\frac{\xi_1}{\xi_0} = \left(\frac{M}{\sqrt{M_p}}\right) \propto \frac{1}{B_v R} \tag{26}$$

This is the same result as obtained in Ref. [4]. From Eq. (25) we can see that although in the non-long-thin case, the displacement has a stronger z dependence, the necessary condition for suppression in the low field region is the same as that in the long-thin case. Namely, the lower limit for $\left(\frac{M}{\sqrt{M_p}}\right) < 1$ is $\beta_o = 50\%$ (when $M \to 1$).

Of course, this critical value for beta is a function of mirror ratio. A higher mirror ratio has more unfavorable curvature and therefore, it is necessary to increase the β to further suppress the displacement in the low field region. Certain β value may be stable for low mirror ratio and unstable for higher mirror ratio. This analysis implies increased stability for a rippled central cell tandem mirror field.

§3 Ripple Stabilization

A rippled axisymmetric mirror configuration (Fig. 1) is a combination of a simple mirror with a series of small mirrors. For a high β plasma with isotropic pressure, it can be stable in the low mirror ratio region (with length of $2L_s$), unstable in the high mirror ratio region (with length of $2(L-L_s)$) and as a whole, marginally stable. For a fixed length ratio, L_s/L, and fixed mirror ratio (B_{m1}/B_o and B_{m2}/B_o), we may ask how many ripples are necessary for stability. As we discussed in §2, for the high β case, the dominant term results from curvature drive, i.e.

$$Q_2 = \int_{-L}^{L} dz \; \frac{2p}{B_v^2} \; \frac{R''}{R} . \tag{27}$$

In order to compensate for the negative integral in the region of $-L \rightarrow -L_s$ and $L_s \rightarrow L$, we would like to examine the scaling of integral $\int_{-L_s}^{L_s} dz \; \frac{2p}{B_v^2} \frac{R''}{R}$ with the number of the ripples. Assuming a sinosoidal field configuration,

$$B_v(z) = \frac{B_o}{2} \{ (M_1 + 1) - (M_1 - 1) \cos \frac{nz}{2L_s} \} \tag{28}$$

We have

$$B_v' (z) = \frac{B_o}{2} (M_1 - 1) \sin\left(\frac{nz}{2L_s}\right) \left(\frac{n}{2L_s}\right) \tag{29}$$

and

$$B_v'' (z) = \frac{B_o}{2} (M_1 - 1) \cos\left(\frac{nz}{2L_s}\right) \left(\frac{n}{2L_s}\right)^2 \tag{30}$$

Here, n is the number of the ripples in the region of $(-L_s \rightarrow L_s)$; M_1 is the mirror ratio of the ripples

$$M_1 = \frac{B_{m1}}{B_o} \tag{31}$$

We notice that all the z - dependence are involved in a form of $\left(\frac{nz}{2L_s}\right)$ and $\frac{R''}{R}$ α n^2. Therefore, the integral

$$\int_{-L_s}^{L_s} dz \; n^2 F\left(\frac{nz}{2L_s}\right)$$

$$= n^2 \int_{-L_s}^{L_s} dx\, F\left(\frac{x}{2L_s}\right) \tag{32}$$

Hence, the scaling with n^2 is very strong and for a fixed length, the more ripples, the greater this stabilizing effect is. However, in a real reactor design, the ripple number is limited by the ripple mirror ratio. Therefore, it is desirable to see the scaling with the ripple mirror ratio, M_1. There are two different cases for $(M_1 - 1) \to 0$ and for finite $(M_1 - 1)$.

When $(M_1 - 1) \to 0$, from eqs. (28), (29) and (30) we have

$$B_v \sim B_o \tag{33}$$

$$B_v' \propto (M_1 - 1) \tag{34}$$

$$B_v'' \propto (M_1 - 1) \tag{35}$$

From Eq. (19), the stabilizing term is proportional to $(\tau^2/2 - \tau')$.

$$\tau^2 \propto (M_1 - 1)^2 \tag{36}$$

The term containing τ',

$$\tau' = \frac{B_v''}{B_v} - \tau^2 \tag{37}$$

involves a term proportional to $(M_1 - 1)$ only. This term changes sign along the path of the integration of (27) causing some cancellation. We thus find the scaling for the term related to $\left(\frac{B_v''}{B_v}\right)$, i.e.

$$\int_{-L_s}^{L_s} dz \; \frac{2p}{B_v^2} \; \frac{B_v''}{B_v} \sim (1 - \frac{1}{M_1^2}) \quad (M_1 - 1)$$

$$\propto (M_1 + 1) \; (M_1 - 1)^2 \tag{38}$$

when $(M_1 - 1) \to 0$, the scaling of $(M_1 + 1)$ is a slowly changing factor. Therefore the contribution to Q_2 from the ripple region is

$$Q_{21} \equiv \int_{-L_s}^{L_s} dz \; \frac{2p}{B_v^2} \; \frac{R''}{R} \propto n^2 (M_1 - 1)^2 \tag{39}$$

Therefore, the greater the ripple mirror ratio, the smaller the necessary number of the ripples is to keep the same value of Q_{21}. However, if $(M_1 - 1)$ increases to a finite number, then the dependence on $(M_1 + 1)$ in (38) becomes important. Since it is the only term which is negative in the integration of (27), the cancellation between this term and the other positive term which are proportional to r^2 will be affected by the $(M_1 + 1)$ scaling. Hence the greater the ripple mirror ratio is, the less the positive value of the integral (39) is. In order to keep the same value of integral Q_{21}, we have to increase the number of the ripples. Therefore, we can expect that there is a specific ripple mirror ratio M_{1c}, at which the necessary number of ripples is minimized. In order to calculate this specific mirror ratio M_{1c}, we developed a new variational form for the basic ballooning equation (1), and did some numerical calculation.

§4 Sturm-Liouville Form

Using the identity in calculus

$$A[B(AD)']' \equiv [ABAD']' + A(BA')'D \tag{40}$$

We can transform the first term in eq. (1) and make eq. (1) into a standard Sturm-Liouville form:

$$[(\Lambda\eta^4 + \frac{Q}{B^2})\,\phi']' + [(\omega^2\frac{\rho}{B^2} - \frac{2p}{B^2}\frac{R''}{R}) + \eta^2\,(\Lambda 2\eta\eta')']\,\phi = 0 \tag{41}$$

By setting

$$\phi = \frac{1}{\eta^2}\,y \tag{42}$$

we may simplify eq. (41) further to

$$\left[\left(\Lambda + \frac{1}{\eta^4}\frac{Q}{B^2}\right)\,y'\right]' + \frac{1}{\eta^2}\left\{\left(\frac{Q}{B^2}\left(\frac{1}{\eta^2}\right)'\right)' + \frac{1}{\eta^2}\left(\frac{\omega^2\rho}{B^2} - \frac{2p}{B^2}\frac{R''}{R}\right)\right\} y = 0 \tag{43}$$

The advantage of this form is that the wall-shape factor Λ is involved in a simple term without any derivative (i.e. Λ') form. When we arrange that the

conducting wall be only in the unfavorable curvature region, this form facilitates the calculation. Using the boundary conditions

$$y' = 0 \text{ at } z = \pm L \tag{44}$$

We can solve eq. (43) by a shooting method for $\omega^2 = 0$. For every given β value, and the ripple amplitude, the number of ripples is adjusted to satisfy the boundary condition at $z = \pm L$. Fig. 2 and Fig. 3 show the results of numerical calculation. The mirror ratio, $\frac{B_{m2}}{B_o}$, is assumed to be 8. The length ratio, $\frac{L_s}{L}$, is assumed to be 0.8. The ratio of the plasma radius to wall radius are assumed to 0.8 (Fig. 2) and 0.9 (Fig.3), respectively. The vacuum magnetic field is a linked sinosoidal form as equation (28). As we analysed in Section 3, the results show a different scaling for $(M_1 - 1) \to 0$ and finite $(M_1 - 1)$ cases. For each given β, there is a critical ripple mirror ratio, at which the necessary ripple number is minimized.

§5 Ripple Formation by Ferromagnetic Rings

Although the most obvious method for creating field ripple would involve properly spaced discrete coils, an alternative appraoch could utilize ferromagnetic rings, which are arranged inside a uniform solenoidal coil to attract the magnetic flux and form a ripple field on axis. Fig. 4 shows the arrangement of ferrmagnetic rings inside a uniform solenoidal coil. The inner radius of ring is determined by the plasma radius and the radial thickness of the halo. The outside radius of ring is limited by the radius of solenoid. The adjustable parameters are the axial thickness of the ring, L_1, the radial thickness, L_2, and the distance between two rings, L_3. For a fixed value of L_2 and L_3, we may change the axial thickness of the ring from 0 to L_3. Apparently, the ripple amplitude will change correspondingly from 0 to some maximum value, then to 0 again. We may also expect that the ripple amplitude will increase with the distance between rings until it approaches a maximum value, but the number of ripples reduces with this distance. We have performed numerical calculation to optimize L_1 and L_3.

For a tandem mirror reactor application, the central cell may be stabilized by the ripples. The central cell magnetic field is about 3 Telsa, which saturates the ferromagnetic rings and facilitates the calculation of the magnetic field. Usually, the magnetic field created by

the ferromagnetic material in the region outside this material can be simulated by current sheets on the surfaces of this material. In the saturated soft iron, this current density is about 1.6×10^4 A/$_{cm}2$[9]. Applying this number on the inner and outer surfaces of rings, we can calculate the ripple field with the EFFI code. Fig. 5 shows typical result of the calculation. The average field is more than 3 Tesla to keep the ferromagnetic ring saturated. The peak that bounds the central cell is created by a "choke" coil that forms a simple mirror with a mirror ratio of about 8. Fig. 6 shows that the ripple amplitude is increasing with the distance L_3. Fig. 7 indicates that the ripple amplitude reaches a maximum between $L_1 = 0$ and $L_1 = L_3$. Based on these calculations, we may select the ripple number of 9 and ripple amplitude of 1.15 for $\beta_o = 0.75$ (β_o is the vacuum beta at the minimum of the magnetic field.) This can be realized by a set of ferromagnetic rings with $L_1 = 0.54$ M, $L_2 = 0.50$ M and $L_3 = 2.0$ M for the central cell of Tara-like reactor (length of central cell is about 20M). The other option is to further reduce the axial thickness of the ferromagnetic ring. In this case, the amplitude of the ripple field is reduced to 1.1; therefore, it cannot stabilize the central cell with $\beta_o = 0.75$. However it can still stabilize the central cell with $\beta_o = 0.80$. The asterisks in Fig. 2, Fig. 3, Fig. 6, and Fig. 7 show the corresponding working points.

Since the ferromagnetic rings are facing the plasma core, the cooling issue and their impact on the tritium breeding ratio must be considered in a reactor design.

§6 Conclusion

It is clear that a self-stabilized high beta central cell is an attractive possibility for a fusion reactor. For an isotropic pressure, a reasonable β_o is about 80% with the wall at $\frac{r_p}{r_w} = 80\%$. It is possible to improve the parameters by adding anisotropic plasma pressure, but it is difficult to create this anisotropy. Therefore, it seems difficult to stabilize the axi-cell by rippling central cell.

Acknowledgements

We are grateful to John Tarrh for his helpful discussion. The numerical calculations of Fig. 2 -6 are helped by Chong-Xin Li. This work is supported by D.O.E. Contract No. DE-AC02-78ET-51013.

Figure Captions

Fig. 1 Rippled axisymmetric mirror configuration.

Fig. 2. Necessary ripple amplitude (M_1 - 1) for stabilization as a function of the number of ripples (For $\frac{r_p}{r_w} = 0.8$).

Fig. 3 Necessary ripple amplitude (M_1 - 1) for stabilization as a function of the number of ripples (For $\frac{r_p}{r_w} = 0.9$).

Fig. 4 The arrangement of ferromagnetic rings inside a uniform solenoid.

Fig. 5. The magnetic field on the axis.

Fig. 6. Ripple amplitude (M_1 - 1) as a function of the distance between two rings.

Fig. 7. Ripple amplitude (M_1 - 1) as a function of the axial thickness of the ring.

Fig. 8 The derivative of angle α in the normal direction.

Fig. 9 A straight field line model for non-long-thin case.

References

[1] H.L. Berk et.al. IAEA-CN-44/C-I-2. Tenth International Conference on Plasma Physics and Controlled Nuclear Fusion Research, London, UK, September 12-19, 1984.

[2] J. Kesner, PFC/JA-84-29, To be published in Nuclear Fusion (1985).

[3] T.B. Kaiser and L.D. Pearlstein, Phys. Fluids 28 (1985), 1003.

[4] X.Z. Li, and J. Kesner, To be published in Nucl. Fusion 25.

[5] X.Z. Li, J. Kesner, and B. Lane, PFC/CP-85-2 submitted to Nucl. Fusion (1985).

[6] L.L. LoDestro, 1985 Sherwood Meeting, Madison, WI.

[7] F.A. Haas and J.A. Wesson, Phys. Fluid, 10, 2245 (1967).

[8] J.P. Freidberg, Review of Modern Physics, 54, 801 (1982).

[9] J. Tarrh, private communication (1985).

Appendix. A Model for Non-long-thin case.

When conducting wall approaches to the plasma surface, the perturbed magnetic field, Q_n, must become zero to keep the variation of vacuum energy finite, i.e.

$$Q_n = (\vec{B} \cdot \nabla)\ (\vec{\xi} \cdot \vec{n}) - (\vec{\xi} \cdot \vec{n})\ \vec{n} \cdot (\vec{n} \cdot \nabla)\ \vec{B} = 0 \qquad \text{(A-1)}$$

Therefore,

$$\frac{1}{\xi_n} \frac{\partial \xi_n}{\partial l} = \vec{n} \cdot (\vec{n} \cdot \nabla)\ \vec{B}$$

$$= \vec{n} \cdot (\vec{n} \cdot \nabla)\ \vec{b} \qquad \text{(A-2)}$$

Here, $\vec{b}$ is the unit vector along the $\vec{B}$ field (Fig. 8). Since only the direction of a unit vector is changing we have

$$\vec{n} \cdot (\vec{n} \cdot \nabla)\ \vec{b} = (\vec{n} \cdot \nabla)\ \alpha \qquad \text{(A-3)}$$

α is the angle between the field line and the axis. After integration of Eq. (A-2), it gives

$$\xi_1 = \xi_o \exp\left\{\int_0^1 dl\ (\vec{n}\cdot\nabla)\ \alpha\right\} \tag{A-4}$$

Here, ξ_o is the initial displacement: l is the length along the field line. When the Q_n at the vacuum plasma surface becomes zero, we would like to calculate the $(\vec{n}\cdot\nabla)\ \alpha$ for the field line on the plasma surface. In the non-long-thin case, it is difficult to calculate the equilibrium; therefore, the analytical solution for α is not available. However, it is still possible to evaluate this integral by a simplified straight field line model (Fig. 9). At region I and III, the field lines are parallel to axis and the long-thin approximation is valid. Hence,

$$B_{pm}^{\ 2} = B_{vm}^{\ 2} - 2\ p_m \tag{A-5}$$

$$B_{po}^{\ 2} = B_{vo}^{\ 2} - 2p_o \tag{A-6}$$

Here, the subscript p and v refer to the plasma and vacuum, respectively, the subscript m and o refer to the peak field and low field points. In the region II, long-thin approximation breaks; then, we assume that the field lines in this region are just the straight line to connect the region I and III. Based on the flux conservation, we can calculate the angles of these straight field lines in the region II.

$$B_{pm} R_m^2 = B_{po} R_o^2 \tag{A-7}$$

$$B_{vm} (r_m^2 - R_m^2) = B_{vo} (r_o^2 - R_o^2) \tag{A-8}$$

Here R_m and R_o are the radius of the plasma surface in the corresponding regions. Introducing two mirror ratios:

$$M \equiv \frac{B_{vm}}{B_{vo}} \tag{A-9}$$

and

$$M_p \equiv \frac{B_{pm}}{B_{po}} \tag{A-10}$$

We have

$$r_o^2 - R_o^2 = M (r_m^2 - R_m^2) \tag{A-11}$$

$$R_o^2 = M_p R_m^2 \tag{A-12}$$

Or

$$r_o = \sqrt{R_o^2 + M (r_m^2 - R_m^2)} \tag{A-13}$$

$$R_m = \sqrt{\frac{1}{M_p}}\, R_o \tag{A-14}$$

Therefore,

$$\lim_{r_m \to R_m} \frac{r_o - R_o}{r_m - R_m} = \lim_{r_m \to R_m} \frac{\sqrt{R_o^2 + M\left(R_m^2 - \frac{1}{M_p} R_o^2\right)} - R_o}{R_m - \frac{1}{M_p} R_o}$$

$$= \frac{1}{2R_o} M \left(R_m + \sqrt{\frac{1}{M_p}}\, R_o\right) = \frac{M}{\sqrt{M_p}} \tag{A-15}$$

On the other hand, from Fig. 9 we have

$$\alpha_v - \alpha_p = \operatorname{arctg}\left(\frac{r_o - r_m}{L}\right) - \operatorname{arctg}\left(\frac{R_o - R_m}{L}\right)$$

$$\to \frac{1}{L}\left\{(r_o - R_o) - (r_m - R_m)\right\} \tag{A-16}$$

and

$$\Delta n_1 = c_1 l + c_2 \tag{A-17}$$

$$c_1 = \frac{(r_o - R_o)\cos\alpha - (r_m - R_m)\cos\alpha}{L/\cos\alpha} = \frac{(r_o - R_o) - (r_m - R_m)}{L} \cos^2\alpha \tag{A-18}$$

$$c_2 = (r_m - R_m) \cos\alpha \tag{A-19}$$

therefore,

$$(\vec{n} \cdot \nabla)\ \alpha \equiv \lim_{\Delta n_1 \to 0} \frac{\alpha_v - \alpha_p}{\Delta n_1}$$

$$= \frac{(r_o - R_o) - (r_m - R_m)}{L} \qquad \frac{1}{(c_1 l + c_2)} \tag{A-20}$$

Thus the integration

$$\int_{l_m}^{l_o} dl\ (\vec{n} \cdot \nabla)\ \alpha = \frac{(r_o - R_o) - (r_m - R_m)}{L} \int_{o}^{L/\cos\alpha} dl \quad \frac{1}{(c_1 l + c_2)}$$

$$= \frac{(r_o - R_o) - (r_m - R_m)}{c_1 L} \log \left[1 + \frac{c_1}{c_2} \frac{L}{\cos\alpha}\right]$$

$$= \frac{1}{\cos^2\alpha} \log \left[\frac{r_o - R_o}{r_m - R_m}\right]$$

$$= \left[\frac{M}{\sqrt{M_p}}\right] \quad \frac{1}{\cos^2\alpha} \tag{A-21}$$

Finally, we have

$$\xi_o = \xi_m \left(\frac{M}{\sqrt{M_p}}\right)^{\cos^{-2}\alpha} \tag{A-22}$$

Now we can see that the suppression of the displacement is stronger in the non-long-thin case, since $\cos^2\alpha < 1$ when $\alpha \neq 0$. It approaches long-thin approximation when $\alpha \to 0$. However, the necessary β_o to have suppression effect is still 50% even if the non-long-thin effect is taken into account. From eq. (A-22), it is necessary to have

$$\left(\frac{M}{\sqrt{M_p}}\right) < 1 \tag{A-23}$$

in order to obtain the suppression effect. When β_o increases, M_p increases to make $M < \sqrt{M_p}$. The smaller the M is, the lower the β_o is. In fact

$$\frac{M}{\sqrt{M_p}} = \left[\frac{M^2\,(1-\beta_o)}{1 - \frac{1}{M^2}\,\beta_o}\right]^{1/4} \tag{A-24}$$

for the case $p_m = p_o$. Then condition (A-23) becomes

$$\beta_o > \frac{1 - \frac{1}{M^2}}{1 - \frac{1}{M^4}} \qquad \text{(A-25)}$$

When $M \rightarrow$, the necessary $\beta_o \rightarrow 1$. When $M \rightarrow 1$

$$\beta_o \rightarrow \frac{1}{2} \qquad \text{(A-26)}$$

This is the same conclusion as long-thin case.

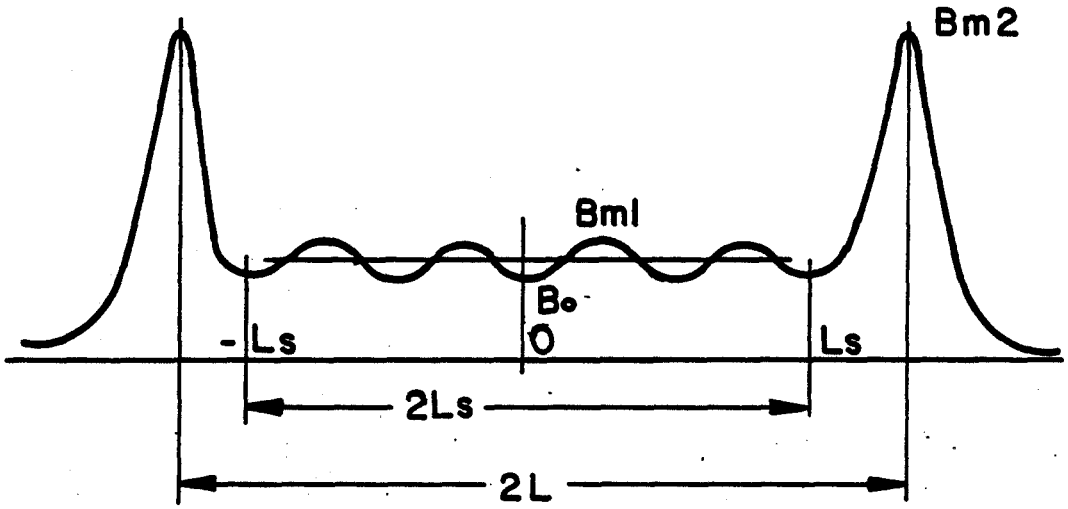

FIG. 1

Rippled Axisymmetric Mirror Configuration

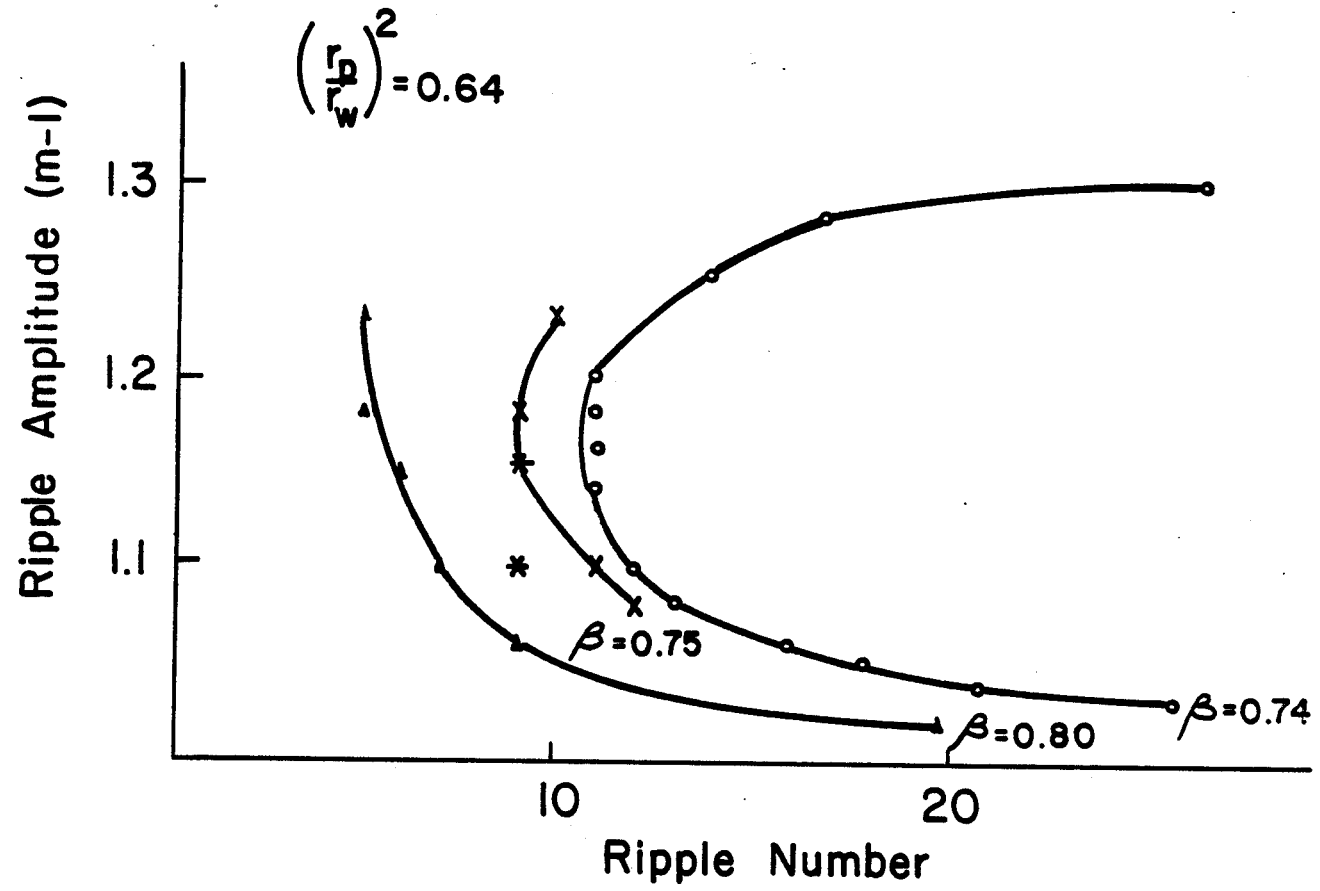
$\left(\frac{r_p}{r_w}\right)^2 = 0.64$
Ripple Amplitude (m-1)
1.3
1.2
1.1
$\beta = 0.75$
$\beta = 0.80$
$\beta = 0.74$
10
20
Ripple Number

FIG. 2

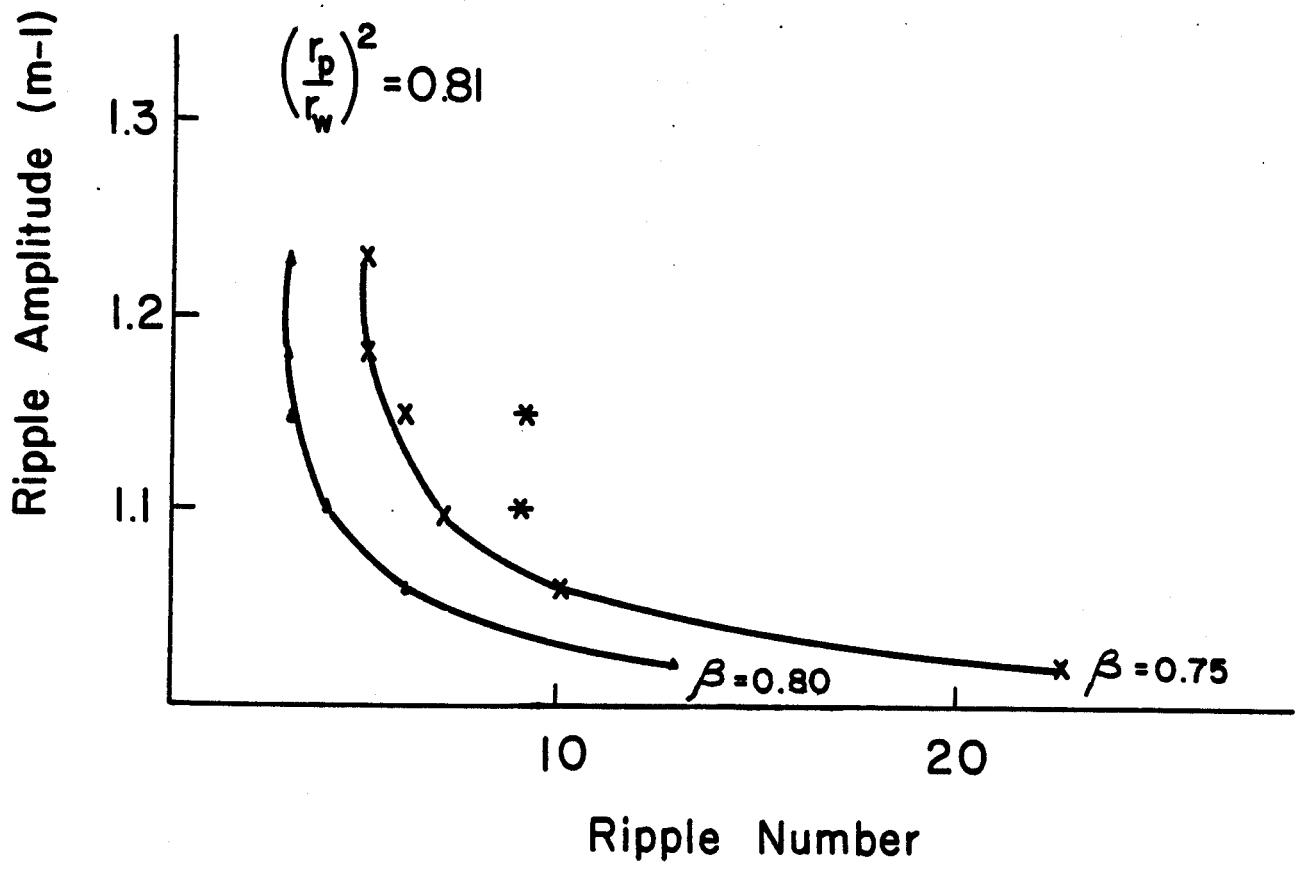
$\left(\frac{r_p}{r_w}\right)^2 = 0.81$
Ripple Amplitude (m-1)
1.3
1.2
1.1
$\beta = 0.80$
$\beta = 0.75$
10
20
Ripple Number

FIG. 3

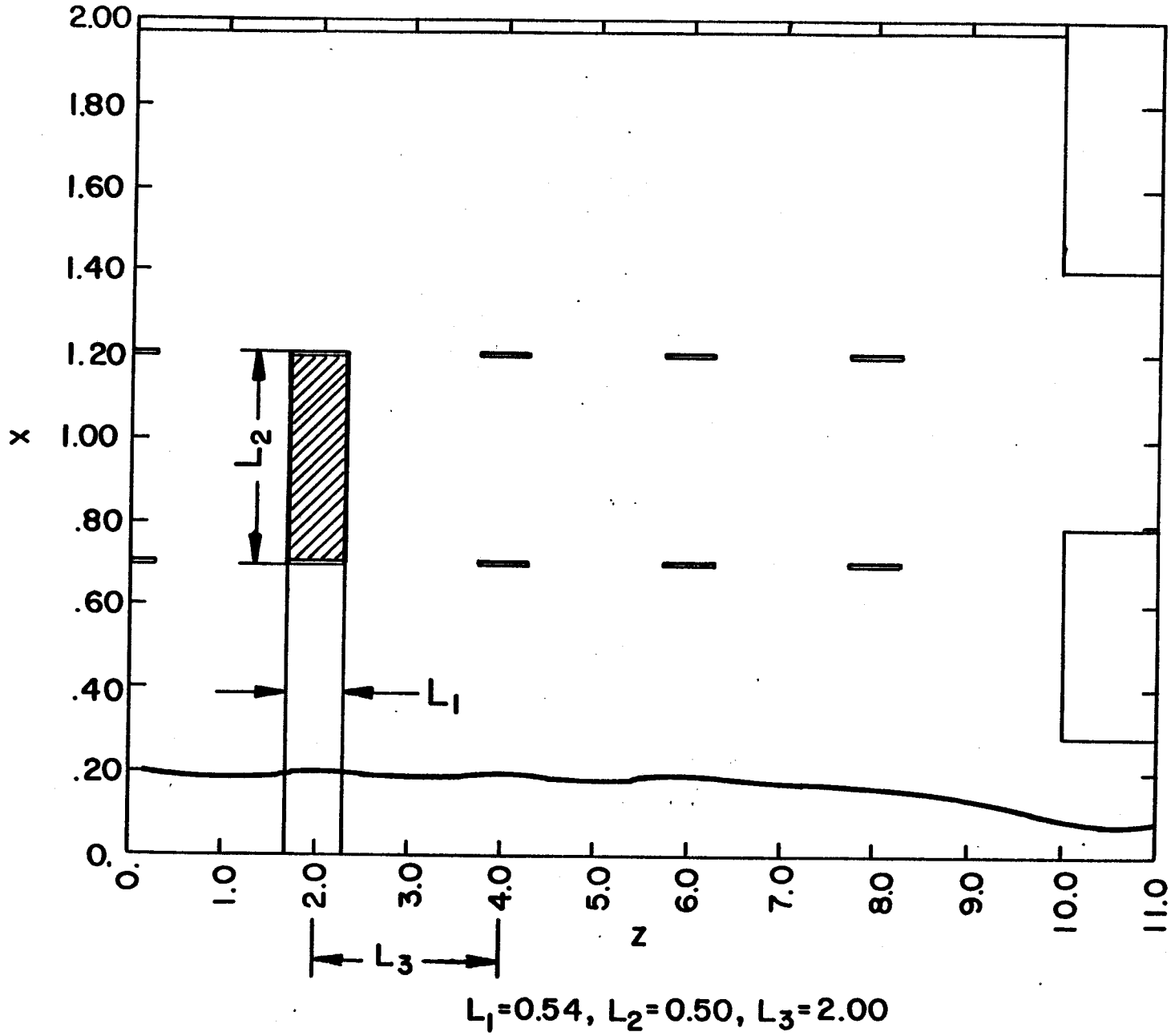
2.00
1.80
1.60
1.40
1.20
1.00
.80
.60
.40
.20
0.
x
L_2
L_1
L_3
0.
1.0
2.0
3.0
4.0
5.0
6.0
7.0
8.0
9.0
10.0
11.0
z
L_1=0.54, L_2=0.50, L_3=2.00

FIG.4

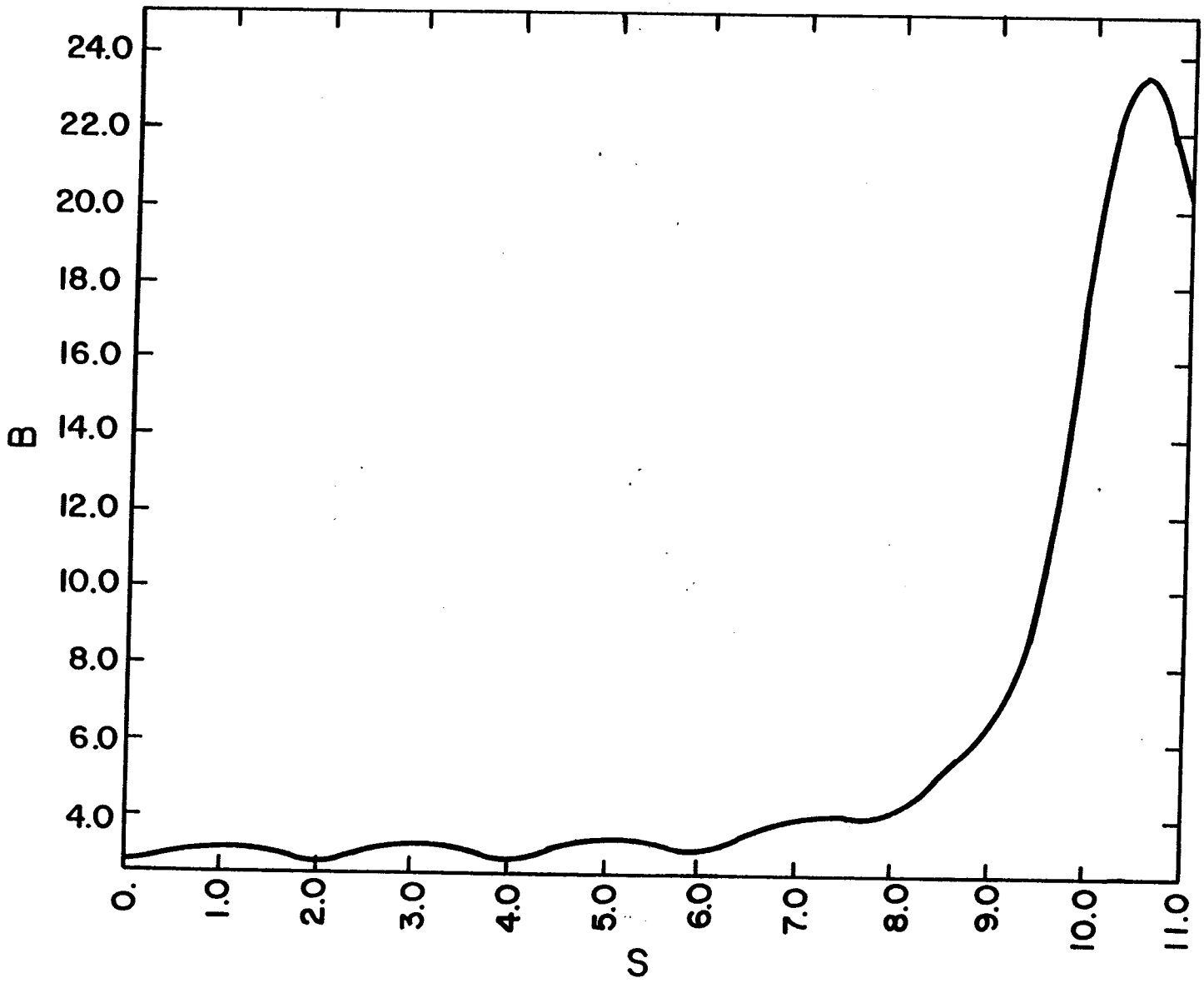
24.0
22.0
20.0
18.0
16.0
14.0
12.0
10.0
8.0
6.0
4.0
B
0.
1.0
2.0
3.0
4.0
5.0
6.0
7.0
8.0
9.0
10.0
11.0
S

FIG. 5

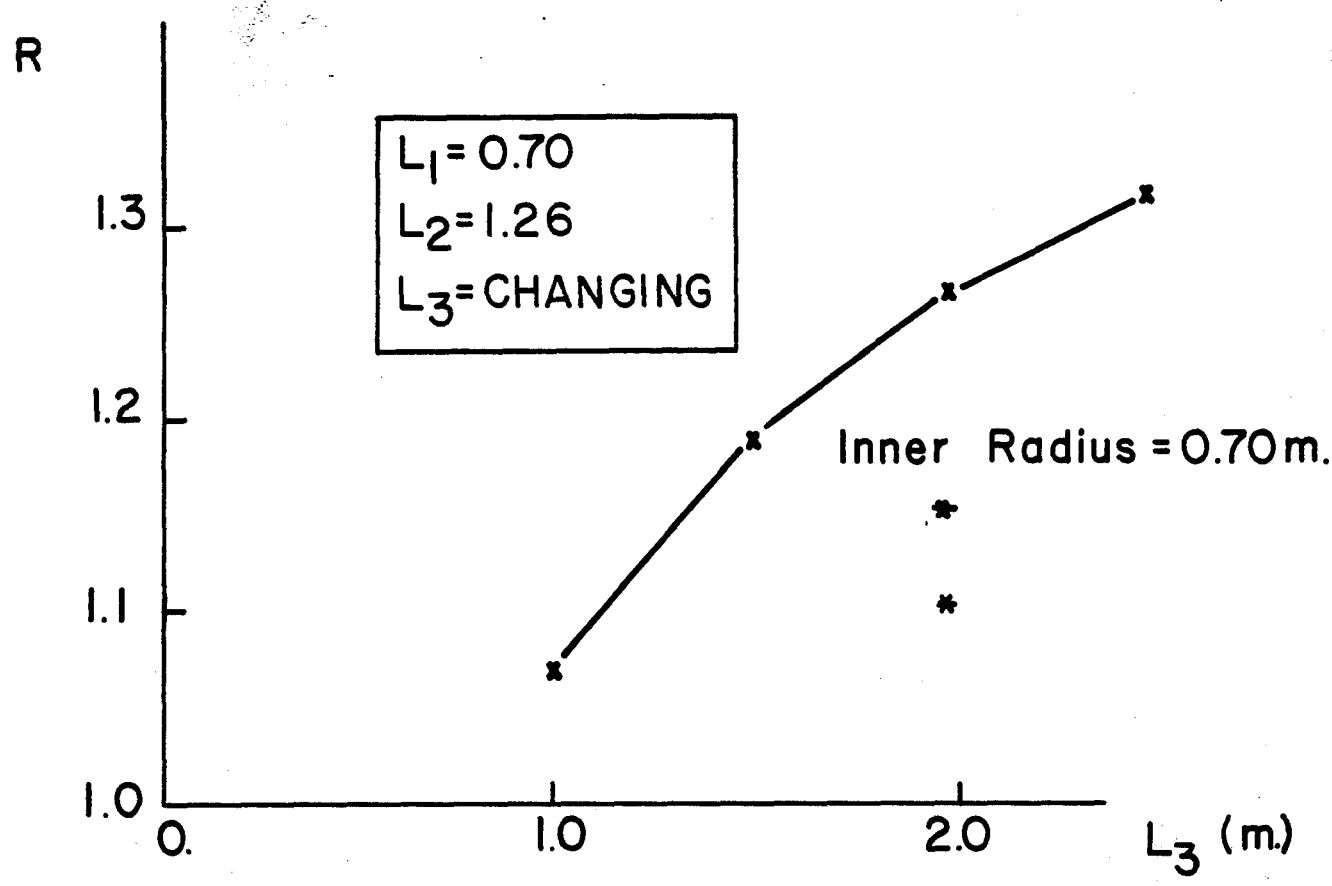
R
1.3
1.2
1.1
1.0
L_1 = 0.70
L_2 = 1.26
L_3 = CHANGING
Inner Radius = 0.70 m.
0.
1.0
2.0
L_3 (m.)

FIG. 6

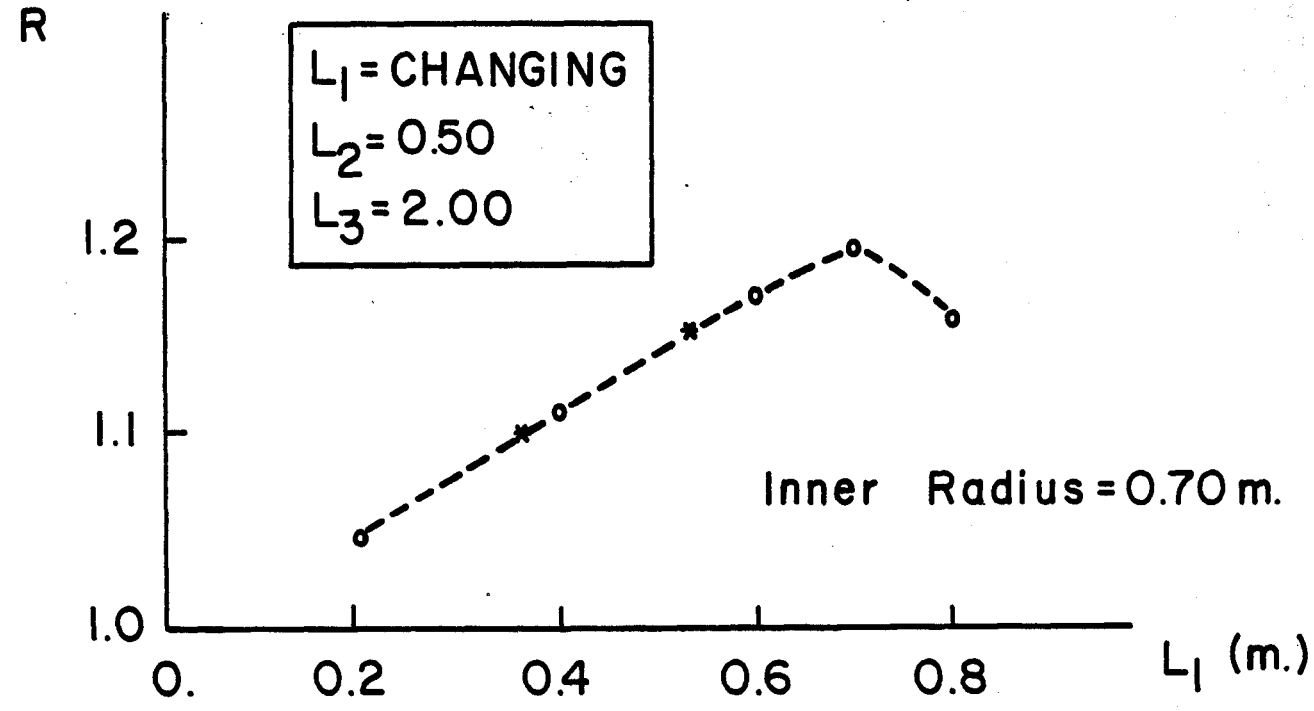
R
1.2
1.1
1.0
L_1 = CHANGING
L_2 = 0.50
L_3 = 2.00
Inner Radius = 0.70 m.
0.
0.2
0.4
0.6
0.8
L_1 (m.)

FIG. 7